

## Electron relaxation in quantum dots by means of Auger processes

U. Bockelmann and T. Egeler

*Walter Schottky Institut, Technische Universität München, Am Coulombwall, D-8046 Garching, Germany*

(Received 4 August 1992)

The present theoretical work deals with the relaxation of hot electrons in quantum dots by Coulomb scattering with an electron-hole plasma. A random-phase approximation is used which includes single-particle and collective-plasma excitations. We discuss the influence of the dot size, plasma density, and temperature. The resulting transition rates are of the order of  $10^{12} \text{ s}^{-1}$  for a plasma density of  $10^{15} \text{ m}^{-2}$  in  $\text{In}_{0.53}\text{Ga}_{0.47}\text{As}/\text{InP}$ . In the presence of a dense electron-hole plasma, hot electrons can relax efficiently by Auger processes, even in small semiconductor quantum dots where the relaxation by phonon scattering is weak.

In recent years, a lot of research activity has been devoted to the optical properties of one- and zero-dimensional semiconductor structures (quantum wires and dots). This is motivated by a fundamental interest in the physics of lower-dimensional systems and by a theoretically predicted increasing performance of optical devices with decreasing dimensionality.<sup>1</sup> Strongly enhanced oscillator strengths<sup>2</sup> and optical nonlinearities<sup>3</sup> as well as higher performance for lasers<sup>4,5</sup> and modulators<sup>6</sup> are expected, in particular for quantum dots where a quantum confinement in all three directions gives rise to a discrete energy spectrum and thus to a strongly peaked density of states. However, there still does not exist any satisfactory method to confine electrons and holes in more than one spatial direction. Usually technological problems are used to explain why the above predictions have not yet been confirmed experimentally. For instance, the luminescence efficiency measured from quantum dot structures is always found to decrease with decreasing dot size.<sup>7-9</sup>

It has been shown theoretically that in zero-dimensional (0D) semiconductor systems electron scattering by acoustical phonons becomes increasingly quenched with an increasing separation of the discrete energy levels.<sup>10,11</sup> The resulting, strongly reduced relaxation of hot carriers is expected to limit the luminescence efficiency of small quantum dots in an intrinsic manner.<sup>12</sup> However, when phonon scattering becomes weak does an alternative, efficient relaxation mechanism exist? This work deals with electronic transitions in quantum dots mediated by the interaction with an electron-hole plasma. Auger processes in 2D and 3D systems have been studied theoretically by several groups.<sup>13-15</sup> Experimentally it has been shown<sup>16,17</sup> that the Coulomb interaction is important for the relaxation of hot carriers at high carrier densities in bulk GaAs. As a high plasma density is quite usual, e.g., during laser operation (typical 2D plasma densities are of the order of  $10^{16} \text{ m}^{-2}$  in quantum well lasers<sup>5</sup>), the present model calculations may contribute significantly to our knowledge about the theoretical limits of optical devices based on quantum dot structures.

The energy structure of a quantum dot consists of low-lying discrete levels which, with increasing energy, evolve to a quasicontinuum of energy states (near and

above the top of the confining potential). We model the discrete, low-energy states by a 0D system and the quasicontinuous high-energy region by a 2D system. This is a well-suited approximation to describe typical luminescence experiments on quantum dots fabricated from quantum wells by lateral patterning techniques. There, electron-hole pairs are created above the barrier of the lateral potential but they are still confined along the growth ( $z$ ) direction within the underlying quantum well. Usually, optical transitions originating from the low-lying (0D) energy states are studied. We calculate the Coulomb scattering between an electron-hole plasma in the 2D region and a single electron in a 0D state. A scattering event involves a transition between two different 0D states and an excitation (deexcitation) of the 2D electron-hole plasma. Carrier exchange between the 0D and 2D systems is neglected. This approximation is justified later in the text. Throughout the work we suppose the electrons and holes to be confined along the  $z$  direction within an unstrained 10-nm-wide  $\text{In}_{0.53}\text{Ga}_{0.47}\text{As}/\text{InP}$  quantum well. The additional, lateral confinement of the 0D system is described by infinite barrier quantum wells of equal width  $L$  along the  $x$  and  $y$  axis. By using a 2D electron-hole plasma we neglect the effect of the lateral potential on the electron and hole continuum states.

We first describe the Coulomb interaction between the 0D system and a 2D electron gas. For an excitation of wave vector  $\mathbf{q}$  (throughout this work, boldface indicates a bidimensional vector, defined in the  $xy$  plane) of the 2D electron gas accompanied by a transition from the 0D state  $i$  to  $j$  ( $i, j$  comprise the lateral quantum numbers of the 0D states) the interaction operator reads

$$\hat{W} = V_{\text{eff}}(\mathbf{q}, i, j) \hat{\rho}_q \hat{c}_j^\dagger \hat{c}_i. \quad (1)$$

Here  $\hat{\rho}$  is the density operator of the 2D electron gas in  $k$  space and the  $c^\dagger, c$  are the creation and annihilation operators for the 0D states. The Coulomb matrix element  $V_{\text{eff}}$  is given by

$$V_{\text{eff}}(\mathbf{q}, i, j) = V_{2D}(q) \int d\mathbf{r} \psi_i(\mathbf{r}) \psi_j(\mathbf{r}) e^{i\mathbf{q}\cdot\mathbf{r}}. \quad (2)$$

The  $\psi$  indicate the lateral ( $x, y$ ) wave functions of the 0D states and  $V_{2D}$  is the 2D Fourier transformation of the

Coulomb potential, screened by the lattice dielectric constant  $\epsilon_l$ ,

$$V_{2D}(q) = \frac{e^2}{2\epsilon_0\epsilon_l Aq} \int dz \int dz' e^{-q|z-z'|} |\chi(z)|^2 |\chi(z')|^2,$$

where  $A$  is the area of normalization of the 2D gas.  $\chi$  is the ground-state wave function of the quantum well in the  $z$  direction. Excited  $z$  subbands are not considered in this work. Typically, they correspond to higher energies than the lateral subbands since the dimension of the quantum dot is smaller in the  $z$  direction than in the lateral directions. In the Born approximation, the rate for Coulomb scattering from the 0D state  $i$  to  $j$  is given by

$$\begin{aligned} \tau_{i,j}^{-1} &= \frac{2\pi}{\hbar} \sum_{m,n,q} |V_{\text{eff}}(\mathbf{q}, i, j)|^2 \langle n | \hat{\rho}_q | m \rangle^2 \\ &\quad \times \delta(E_n - E_m - \hbar\omega_{ij}) e^{-\beta E_m} / Z \\ &= \hbar^{-2} \sum_q |V_{\text{eff}}(\mathbf{q}, i, j)|^2 S(q, \omega_{ij}), \end{aligned} \quad (3)$$

where  $E_m$  ( $E_n$ ) is the energy of the initial state  $m$  (final state  $n$ ) of the interacting 2D electron gas,  $\hbar\omega_{ij}$  is the energy separation between the 0D levels  $i$  and  $j$ ,  $\beta = (kT)^{-1}$ , and  $Z$  is the partition function. The dynamical structure factor  $S$  is related to the retarded irreducible polarizability  $\Pi$  of the 2D electron gas by<sup>18</sup>

$$\begin{aligned} S(q, \omega) &= \int dt e^{-i\omega t} \langle \langle \hat{\rho}_q^\dagger \hat{\rho}_q(t) \rangle \rangle \\ &= \frac{2\hbar}{1 - e^{-\beta\hbar\omega}} \frac{\text{Im}[\Pi(q, -\omega)]}{|\epsilon(q, -\omega)|^2}. \end{aligned} \quad (4)$$

The double angular brackets indicate the quantum statistical average. The dielectric function  $\epsilon$  reads

$$\epsilon(q, \omega) = 1 - \Pi(q, \omega) V_{2D}(q). \quad (5)$$

The precision of the calculation is determined by the approximation used for the polarizability  $\Pi$ . We employ the random-phase approximation (RPA), for which  $\Pi$  can be expressed analytically at zero temperature.<sup>19</sup> The finite-temperature polarizability is calculated from the zero-temperature result using Maldague's method.<sup>20</sup> The electron-hole plasma is described as a three-component plasma consisting of electrons, heavy holes, and light holes. We neglect transitions between the three plasma components and the heavy-hole-light-hole mixing. Under these approximations, the Coulomb interaction with the electron-hole plasma is described by Eqs. (3)–(5), where  $\Pi$  is the sum of the RPA polarizabilities of the three plasma components.<sup>21</sup>

Figure 1 shows the dependence of the Coulomb scattering rate on the lateral size  $L$  of the quantum dot at a plasma density  $n$  of  $2 \times 10^{15}$  pairs/m<sup>2</sup>. The solid, dotted, and dashed lines are calculated by introducing  $\epsilon(q, \omega)$ ,  $\epsilon(q, 0)$ , and  $\epsilon = 1$  into Eq. (4). We thus compare the dynamically screened, the statically screened, and the unscreened Coulomb interaction, respectively. Each of the three curves exhibits a maximum. The dynamical result is similar to the unscreened (statically screened) result for level separations  $\hbar\omega_{21}$  well above (below) the quasi-Fermi-energies of the plasma components (in the present

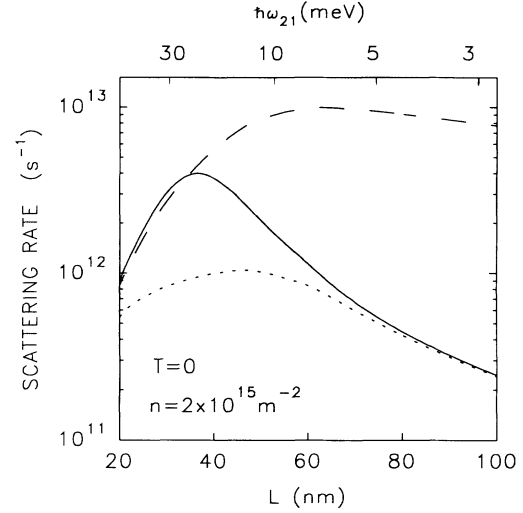


FIG. 1. Coulomb scattering rate  $\tau_{21}^{-1}$  (from the first excited to the ground state 0D level) as a function of the lateral size  $L$  of the quantum dot. The upper scale shows the corresponding separation of the 0D energy levels. Solid, dotted, and dashed lines indicate a dynamical screened, a statically screened, and an unscreened interaction, respectively.

case,  $E_F$  equals 11.7 meV for the electrons and 7.3 meV for the heavy holes, while the light-hole states are still unoccupied). The decrease of the scattering rate  $\tau_{21}^{-1}$  with  $\hbar\omega_{21}$  below about 7 meV is mainly due to the shrinkage of the energy shells around the electron and the hole Fermi energies available to inelastic scattering with decreasing scattering energy. In this regime ( $\hbar\omega_{21} < E_F$ ) screening is important but can be described statically and therefore a single-particle picture can be employed. The decrease of  $\tau_{21}^{-1}$  with the lateral dot size  $L$  below about 40 nm is an effect of the Coulomb matrix element  $V_{\text{eff}}$ . Figure 2 (top part) shows that the relevant matrix element exhibits a maximum with respect to the wave vector  $q$  at about  $q = \pi/L$  which strongly broadens and decreases with decreasing  $L$ . In the bottom part of Fig. 2 we have plotted the dynamical structure factor  $S$  (normalized to the sample area  $A$ ), calculated with the full  $\epsilon(q, \omega)$ . The solid curve ( $L = 50$  nm) clearly shows the acoustic and the optical plasmon of the 2D electron-hole plasma (at  $q = 6.4 \times 10^7$  and  $2.9 \times 10^7$  m<sup>-1</sup>, respectively). Their dispersion relations start at the origin (zero wave vector and energy), in contrast to the 3D case where a lower-energy threshold exists for the optical plasmon. For  $L = 50$  nm the collective excitations are important in the wave-vector regime where the Coulomb matrix element is sizable while the single-particle excitations clearly dominate the dynamical structure factor  $S$  for  $L = 20$  and 100 nm. Thus, dynamical effects are especially important in the intermediate energy range ( $\hbar\omega_{21} \cong E_F$ ). This is reflected in Fig. 1 by the strong difference between the dynamical (solid) and the static (dotted and dashed) results for  $L$  between 40 and 60 nm. All the following results are calculated by using the dynamical RPA.

In Fig. 3, the density dependence of the scattering rate is plotted for three different values of the lateral size  $L$  of the quantum dot. At low densities (below the maxima),

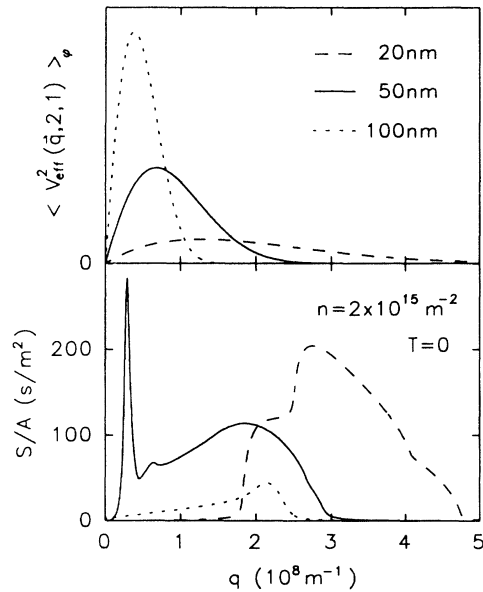


FIG. 2. Coulomb matrix element (top) and dynamical structure factor  $S$  (bottom) as a function of the modulus of the 2D wave vector  $q$ .  $\langle V_{\text{eff}}^2(\mathbf{q}, 2, 1) \rangle_{\varphi} = q \int d\varphi V_{\text{eff}}^2(\mathbf{q}, 2, 1)$  with  $\mathbf{q} = q(\cos\varphi, \sin\varphi)$ . For the calculation of  $S$  a broadening of 1 meV has been assumed (Ref. 22).

the scattering rate increases strongly with increasing plasma density  $n$  and dot size  $L$ . Again this can be understood in a single-particle picture. Since  $\hbar\omega_{21} > E_F$ , the number of initial states available to scattering increases with the area of the Fermi circles and hence the density. The dependence on dot size is governed by the Coulomb matrix element, as described above. The scattering rates pass a maximum in  $n$  when the corresponding Fermi energies are of the order of the energy separation  $\hbar\omega_{21}$  and hence the coupling to single particle as well as collective plasma excitations is efficient. For densities above  $10^{16} \text{ m}^{-2}$ , the light-hole component starts to be populated and a second maximum shows up. In the whole density range discussed here, the calculated Coulomb scattering times

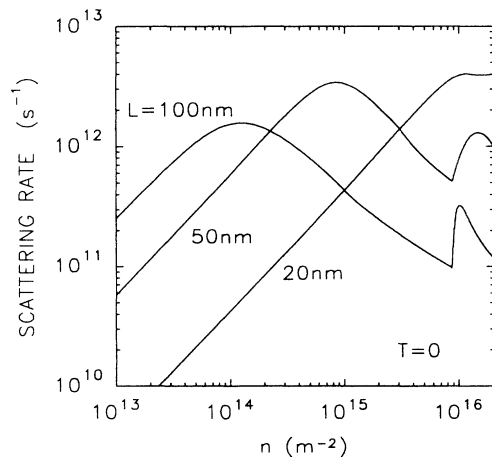


FIG. 3. Scattering rate  $\tau_{21}^{-1}$  as a function of the density  $n$  of electron-hole pairs.

are clearly shorter than the LA-phonon scattering times which in small  $\text{In}_{0.53}\text{Ga}_{0.47}\text{As}/\text{InP}$  quantum dots are longer than a nanosecond.<sup>10</sup>

We should notice that the RPA is a high-density approximation, which is valid for a plasma parameter  $r_s$  smaller than one. In the present system, the 2D densities corresponding to  $r_s = 1$  are  $9.6 \times 10^{14} \text{ m}^{-2}$  for the electrons and  $2.5 \times 10^{15} \text{ m}^{-2}$  for the heavy holes. For densities below  $10^{15} \text{ m}^{-2}$  the calculations should thus be considered with some reserve. In addition, for real structures carrier localization at potential fluctuation can be important at low densities. Nevertheless, we do not expect important changes of the present results in the low-density region, since, as described above, for  $\hbar\omega_{21} \gg E_F$  the scattering rates are mainly determined by the interplay of the Coulomb matrix element and the single-particle excitations of the 2D plasma and not by collective effects.

Up to now we have discussed the zero-temperature case. There, energy is always transferred from the 0D system into the 2D plasma. The discussed scattering rate  $\tau_{21}^{-1}$ , decreases slightly with increasing temperature, as shown in Fig. 4 (curve labeled  $2 \rightarrow 1$ ). This is due to an increasing thermal broadening of the dynamical structure factor  $S$  to larger  $q$  values where the Coulomb matrix element is weak (Fig. 2). Coulomb scattering from lower to higher 0D levels becomes increasingly important with temperature. Such processes involve an energy transfer from the thermally excited electron-hole plasma into the 0D system. In Fig. 4, the curves labeled  $1 \rightarrow *$  and  $2 \rightarrow *$  show the total scattering rates (the sum over the scattering rates to all 0D levels above or below the initial level) of the ground and the first excited state. When the thermal energy  $kT$  increases above the energy separations of the 0D levels the overall scattering rates increase strongly and the 0D electron experiences an energy gain in average.

We have seen that Coulomb scattering can lead to an efficient energy transfer between the 0D system and the

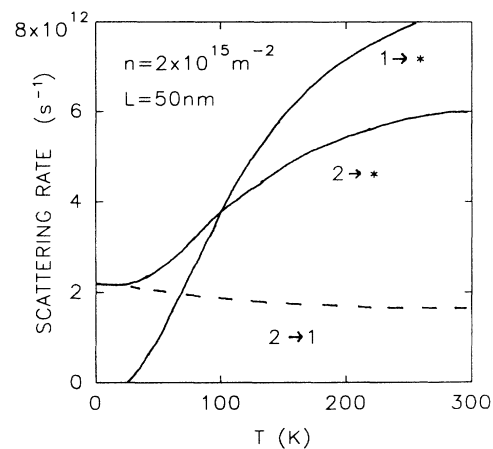


FIG. 4. Total scattering rate from the lowest ( $1 \rightarrow *$ ) and from the first excited ( $2 \rightarrow *$ ) 0D state and the rate  $\tau_{21}^{-1}$  of scattering from the first excited to the ground state ( $2 \rightarrow 1$ ) as a function of the temperature  $T$ .

electron-hole plasma. We thus expect a fast relaxation of excited carriers in quantum dots in the presence of a high-density plasma that itself exhibits an efficient energy exchange with the phonon bath.

Auger processes can also mediate the capture of electrons and holes from the plasma into the 0D system. We study such capture for the electrons by replacing the initial 0D state in Eq. (2) by a 2D plane wave that we orthogonalize to the localized states of the 0D system (OPW). The rate of capture into a given 0D state is then obtained from Eq. (3) with an additional summation performed over the 2D wave vector of the OPW. The calculations of the capture rates contain one more parameter: the energy difference  $E_c$  between the bottoms of the 0D and the 2D system (the depth of the quantum dot). The OPW is orthogonal to all 0D states of confinement energy below  $E_c$ . For  $E_c = 100$  meV,  $n = 2 \times 10^{15} \text{ m}^{-2}$ ,  $L = 50$  nm, and  $T = 0$ , we obtain a capture rate of  $1.7 \times 10^{10} \text{ s}^{-1}$  ( $2.0 \times 10^{11} \text{ s}^{-1}$ ) into the ground (first excited) state, small

values compared to the scattering rates between the 0D levels, discussed above. This somewhat justifies the approximation of a zero carrier exchange between the 0D and 2D system. The large majority of the 2D carriers enter the 0D system from the top and descend the staircase of discrete energy levels.

In conclusion, we have studied a theoretical model of a quantum dot in the presence of an electron-hole plasma. For sizable plasma densities, Auger processes are efficient and represent the dominant relaxation mechanism. The electron-phonon interaction is not necessarily a limiting factor for the possible use of optically active devices based on quantum dot structures.

Many thanks to G. Abstreiter, G. Bastard, J. A. Brum, M. Haines, D. Oberli, B. Vinter, and P. Vogl for valuable discussions. This work has been partly supported by the Deutsche Forschungsgemeinschaft (SFB348) and by a PROCOPE contract.

<sup>1</sup>For an overview see C. Weisbuch and B. Vinter, *Quantum Semiconductor Structures* (Academic, New York, 1991), Chap. VI.

<sup>2</sup>G. W. Bryant, Phys. Rev. B **37**, 8763 (1988).

<sup>3</sup>S. Schmitt-Rink, D. A. B. Miller, and D. S. Chemla, Phys. Rev. B **35**, 8113 (1987).

<sup>4</sup>Y. Arakawa and H. Sakaki, Appl. Phys. Lett. **40**, 939 (1982).

<sup>5</sup>Y. Arakawa and A. Yariv, IEEE J. Quantum Electron. **QE-22**, 1887 (1986).

<sup>6</sup>I. Suemune and L. A. Coldren, IEEE J. Quantum Electron. **QE-24**, 1778 (1988).

<sup>7</sup>E. M. Clausen, Jr., H. G. Craighead, J. P. Harbison, A. Scherer, L. M. Schiavone, B. Van der Gaag, and L.T. Florez, J. Vac. Sci. Technol. B **7**, 2011 (1989).

<sup>8</sup>C. M. Sotomayor Torrès, P. D. Wang, W. E. Leitch, H. Benisty, and C. Weisbuch, in *Optics of Excitons in Confined Systems*, edited by A. Quattropani (Institute of Physics, London, 1991).

<sup>9</sup>A. Schmidt, A. Forchel, J. Straka, I. Gyuro, P. Speier, and E. Zielinski, J. Vac. Sci. Technol. B (to be published).

<sup>10</sup>U. Bockelmann and G. Bastard, Phys. Rev. B **42**, 8947 (1990).

<sup>11</sup>U. Bockelmann, in *Intersubband Transitions in Quantum Wells*, edited by E. Rosencher, B. Vinter, and B. F. Levine (Plenum, New York, 1992), p. 105.

<sup>12</sup>H. Benisty, C. M. Sotomayor-Torrès, and C. Weisbuch, Phys. Rev. B **44**, 10945 (1991).

<sup>13</sup>G. F. Giuliani and J. J. Quinn, Phys. Rev. B **26**, 4421 (1982).

<sup>14</sup>J. F. Young, P. J. Kelly, and N. L. Henry, Semicond. Sci. Technol. **B 7**, 148 (1992).

<sup>15</sup>B. Yu-Kuang Hu and S. das Sarma, Semicond. Sci. Technol. **B 7**, 305 (1992).

<sup>16</sup>J. Shah, B. Deveaud, T. Samen, W. Tsang, A. Gossard, and P. Lugli, Phys. Rev. Lett. **59**, 2222 (1987).

<sup>17</sup>W. Hackenberg, G. Fasol, and H. Kano, Semicond. Sci. Technol. **B 7**, 26 (1992).

<sup>18</sup>D. N. Zubarev, Usp. Fiz. Nauk **71**, 71 (1960) [Sov. Phys. Usp. **3**, 320 (1960)]

<sup>19</sup>F. Stern, Phys. Rev. Lett. **18**, 546 (1967).

<sup>20</sup>P. F. Maldague, Surf. Sci. **73**, 296 (1978).

<sup>21</sup>R. Zimmermann, *Many Particle Theory of Highly Excited Semiconductors* (Teubner, Leibzig, 1988), Chap. III.

<sup>22</sup>N. D. Mermin, Phys. Rev. B **1**, 2362 (1970).